Electronic Supplementary Information

Dual-emissive nanocomposites based on Eu(III) functionalized Cu(I)-coordination polymer for ratiometric fluorescent sensing and integrating Boolean logic operations

Xubin Zheng,[a] Ruiqing Fan,*[a] Kai Xing,[a] Ani Wang,[a] Xi Du,[a] Ping Wang[a] and Yulin Yang*[a]

[a] *MIIT Key Laboratory of Critical Materials Technology for New Energy Conversion and Storage, School of Chemistry and Chemical Engineering, Harbin Institute of Technology, Harbin 150001, P. R. of China*

*Corresponding Author: Ruiqing Fan and Yulin Yang

E-mail: fanruiqing@hit.edu.cn and ylyang@hit.edu.cn

Experimental

Materials and methods

All reagents and solvents were purchased from commercial sources and were used without further purification. Elemental analyses were carried out on a Perkin–Elmer 2400 automatic analyzer. FT–IR spectra data (4000–400 cm^{-1}) were collected by a Nicolet impact 410 FT–IR spectrometer. Scan electron microscope (SEM) images were recorded by Rili SU 8000HSD Series Hitachi New Generation Cold Field Emission SEM. The emission properties were recorded with Edinburgh FLS 920 fluorescence spectrometer equipped with a Peltier-cooled Hamamatsu R928 photomultiplier tube. An Edinburgh Xe900 450 W xenon arc lamp was used as an exciting light source. Thermal analysis was performed on a ZRY-2P thermogravimetric analysis from 30 to 700 °C with a heating rate of 10 °C min^{-1} under a flow of air. Powder X-ray diffraction (PXRD) patterns were recorded in the 2θ range of 5 – 50° using Cu Kα radiation with a Shimadzu XRD-6000 X-ray diffractometer. Elemental analyses for Cu and Eu were conducted using a Perkin-Elmer Model Optima 3300 DV ICP spectrometer. Density functional theory (DFT) calculations were conducted by using the B3LYP/lanl2dz basis set implemented in the Gaussian 09 package. XPS experiments were carried out on a RBD upgraded PHI-5000C ESCA system (Perkin Elmer) with Mg Kα radiation (hv = 1253.6 eV).

Synthesis of [Cu^I(cbpp)(Hcbpp)]·3H_2O (Cu-COOH)

The mixture of CuI (0.05 mmol, 10 mg), Hcbpp (1-(4-carboxylbenzyl)-3-(pyrzin-2-yl) (0.1 mmol, 28 mg) and Na_2SO_3 (0.2 mmol, 25 mg) in 6 mL component solvent (CH_3CN: H_2O=1:1) was placed in a Teflon-lined autoclave (25 mL), sealed, and heated to 120 °C for 3 days. After the autoclave was cooled to room temperature at 10 °C·h^{-1}, red block-shaped crystals suitable for single crystal X-ray crystallographic analysis were obtained. The mother liquor was decanted, and the crystals were rinsed three times with methanol and dried in air for 2 h. Yield: ≈60 % (based on CuI); IR (KBr): 3116(m), 1704(vs), 1618(vs), 1490(m), 1420(m), 1332(m), 1288(m), 1239(m), 1182(m), 1150(vs), 1077(m), 1039(m), 940(m), 859(s), 785(vs), 716(vs), 611(w), 548(w), 511(w), 461(w), 418(w); Elemental analysis calcd (%) for $C_{30}H_{29}CuN_8O_7$: C 53.16, H 4.28, N 16.54; found: C 53.17, H 4.28, N 16.53.

Preparation of Eu(III)@Cu-COOH

Eu(III)@Cu-COOH was prepared by immersing the Cu-COOH (100 mg) in aqueous nitrate salts solution of $Eu(NO_3)_3 \cdot 6H_2O$ (0.1 mol·L^{-1}) and heated to 80 ^{o}C for 12 h. Subsequently, the sample was washed with distilled water three times to remove redundant Eu(III) ions on the surface. Finally, the product was collected by filtration and dried at 60 °C in air. The yield of the Eu(III)@Cu-COOH product based on Cu-COOH was 75.6%.

Preparation of Eu(III)@Hcbpp

The mixture of $Eu(NO_3)_3 \cdot 6H_2O$ (0.1 mmol, 44 mg) and Hcbpp (0.4 mmol, 112 mg) was dissolved in component solvent (CH_3CN: H_2O=1:4) and heated to 80 °C for 12 h. Subsequently, the solvent was removed and the residue was washed with distilled water three times to remove redundant Eu(III) ions on the surface. Finally, the product was collected by filtration and dried at 60 °C in air. The yield of the Eu(III)@Hcbpp product based on Hcbpp was 56.4%.

Fluorescent sensing experiments

For the experiments of sensing various biologically species, powder samples of Eu(III)@Cu-COOH (3 mg) were introduced into HEPES buffer (3 mL) (10 mM, pH=7.4) of AA/H_2O_2, H_2S and Fe(II), respectively. The mixtures were subsequently shaken to form suspensions for luminescent measurements. All the Fluorescence spectra were measured in HEPES buffer (10 mM, pH = 7.4) at an excitation of 330 nm.

Table S1 Crystal data and structure refinement parameters of Cu-COOH

Identification code	Cu-COOH
Empirical formula	$C_{30}H_{29}CuN_8O_7$
CCDC	1587111
Formula mass	677.15
Crystal system	Monoclinic
Space group	$P\,2_1/c$
a (Å)	14.088(5)
b (Å)	20.940(7)
c (Å)	11.306(4)
α (°)	90.00
β (°)	113.423(4)
γ (°)	90.00
V (Å^3)	3060.5(17)
Z	4
D_c/(g cm^{-3})	1.470
μ (Mo Kα)/mm^{-1}	0.775
F(000)	1400
θ range (°)	1.85 – 25.00
Limiting indices	$-16 \le h \le 15$
	$-24 \le k \le 24$
	$-13 \le l \le 12$
Data/Restraints/Parameters	5382 / 0 / 415
GOF on F^2	1.078
R_1[a]	0.0429
wR_2[b]	0.1410
R_1	0.0601
wR_2	0.1520

[a] $R_1 = \Sigma||F_o| - |F_c||/\Sigma|F_o$; [b] $wR_2 = [\Sigma[w(F_o^2 - F_c^2)^2] / \Sigma[w(F_o^2)^2]]^{1/2}$.

Table S2 Selected bond lengths (Å) and bond angles (°) for Cu-COOH

Cu-COOH			
Cu(1)-N(2)	2.044(2)	N(7)-Cu(1)-N(2)	133.89(9)
Cu(1)-N(3)	2.046(2)	N(7)-Cu(1)-N(3)	124.19(8)
Cu(1)-N(6)	2.077(2)	N(2)-Cu(1)-N(3)	80.67(8)
Cu(1)-N(7)	2.020(2)	N(7)-Cu(1)-N(6)	80.17(9)
		N(2)-Cu(1)-N(6)	118.81(9)
		N(3)-Cu(1)-N(6)	125.74(9)

Table S3 Standard deviation calculation

No.	Fluorescence intensity (I_{616})	Fluorescence intensity (I_{485})	I_{616}/I_{485}
1	2515.62 a.u.	7769.34 a.u.	3.088439
2	2500.23 a.u.	7748.89 a.u.	3.099271
3	2507.66 a.u.	7760.78 a.u.	3.094829
4	2499.77 a.u.	7751.23 a.u.	3.100777
5	2512.39 a.u.	7766.56 a.u.	3.091304
Average Value	--	--	3.094924
Standard Deviation (σ)	--	--	0.000591
Slope (*S*) for AA	--	--	0.00394μM^{-1}
Detection limit (3σ/S) for AA	--	--	0.45 μM
Slope (*S*) for H_2S	--	--	0.00162μM^{-1}
Detection limit (3σ/S) for H_2S	--	--	1.09 μM
Slope (*S*) for Fe(II)	--	--	0.0103μM^{-1}
Detection limit (3σ/S) for Fe(II)	--	--	0.17μM

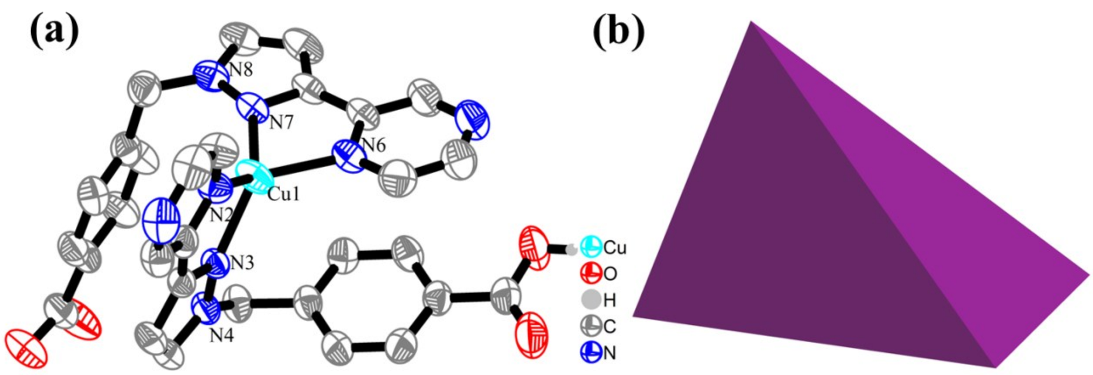

Fig. S1 (a) The structural unit of Cu-COOH with labeling scheme and 50% thermal ellipsoids (hydrogen atoms are omitted for clarity). (b) A distorted tetrahedron.

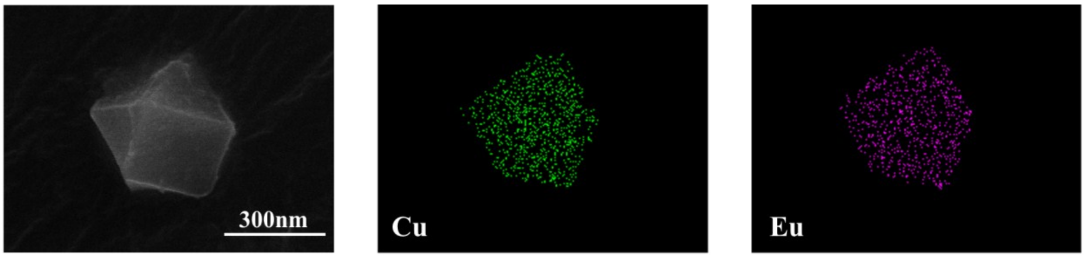

Fig. S2 SEM images for Eu(III)@Cu-COOH, corresponding to the elemental mapping image of Eu(III)@Cu-COOH for the copper element and the europium element.

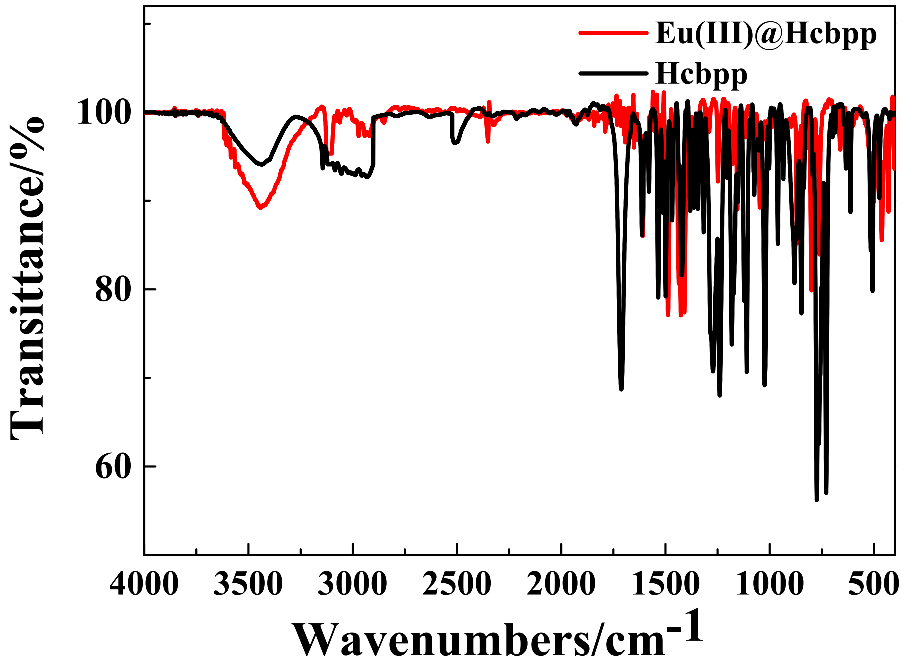

Fig. S3 IR spectra of Hcbpp and Eu(III)@Hcbpp.

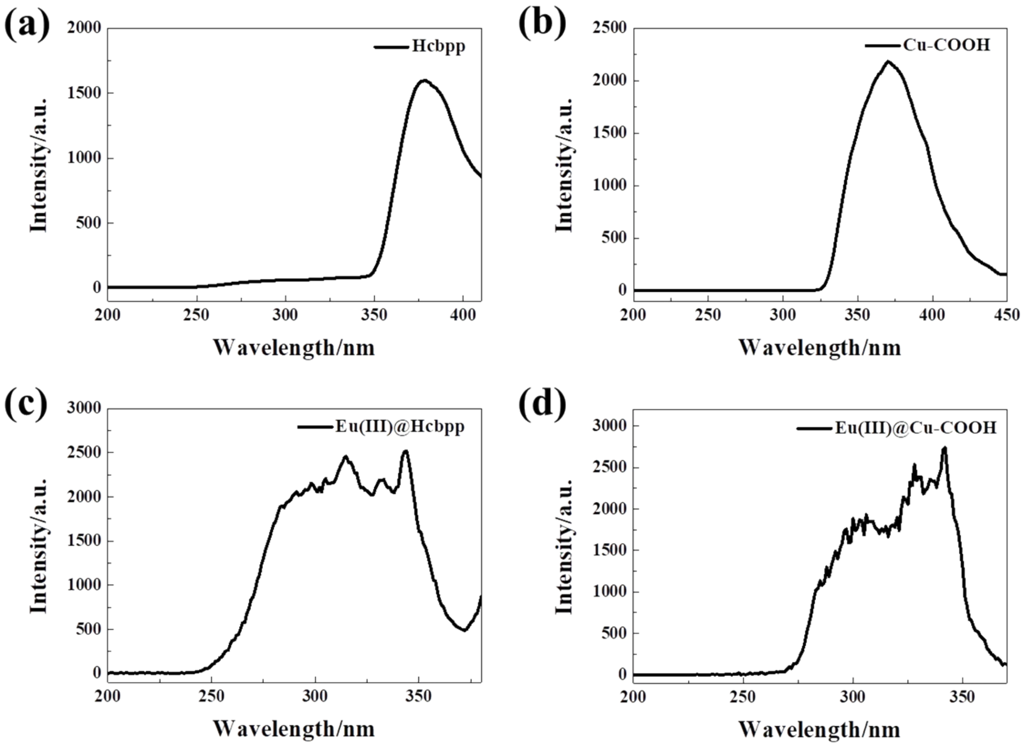

Fig. S4 The excitation spectra of (a) Hcbpp, (b) Cu-COOH, (c) Eu(III)@Hcbpp and (d) Eu(III)@Cu-COOH.

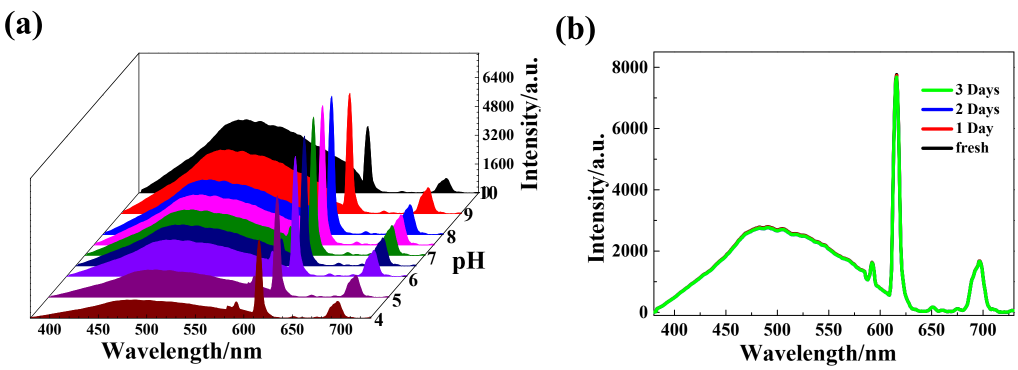

Fig. S5 (a) Fluorescence spectra of Eu(III)@Cu-COOH with the pH varying from 4 to 10. (b) Fluorescence stability of Eu(III)@Cu-COOH.

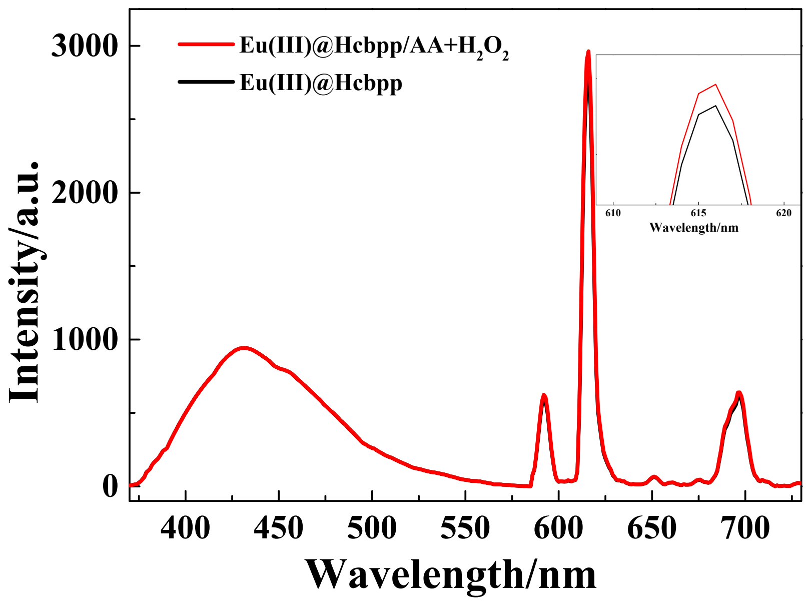

Fig. S6 Fluorescence spectra of Eu(III)@Hcbpp and Eu(III)@Hcbpp with AA/H_2O_2.

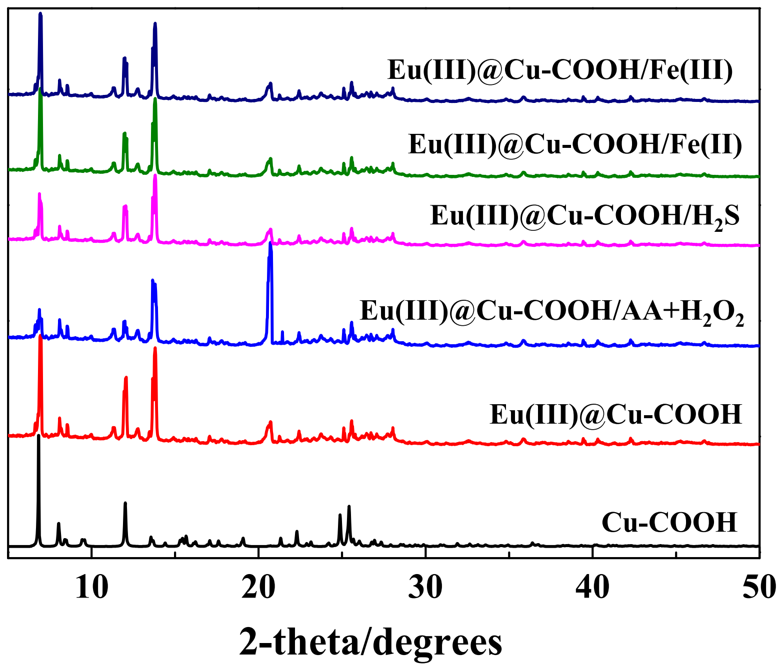

Fig. S7 PXRD patterns of Eu(III)@Cu-COOH after the inclusion of AA/H_2O_2, H_2S, Fe(II) and Fe(III).

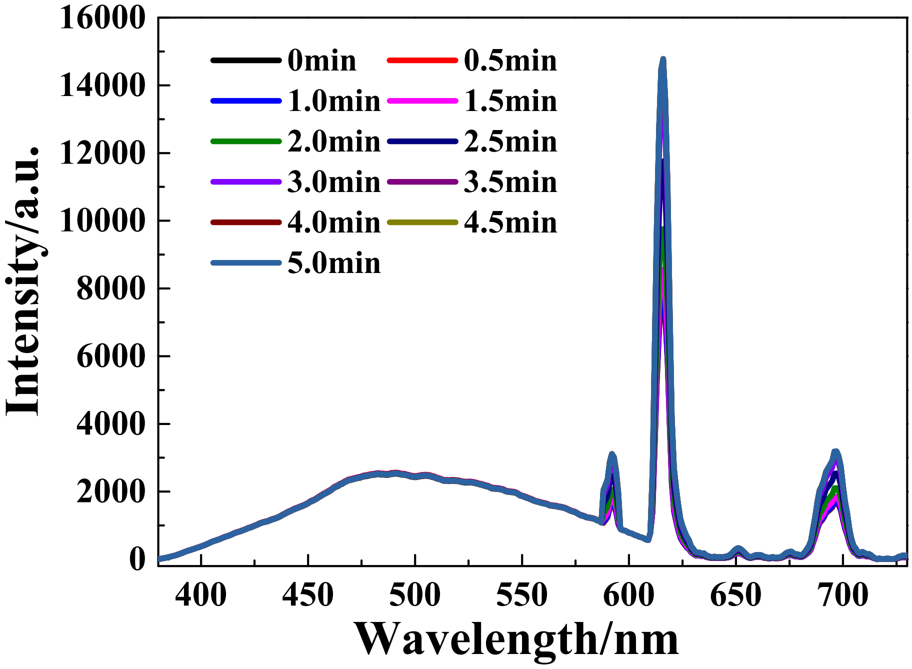

Fig. S8 Fluorescence spectra of Eu(III)@Cu-COOH towards addition of AA/H_2O_2 (2/10 mM) after 0-5 min.

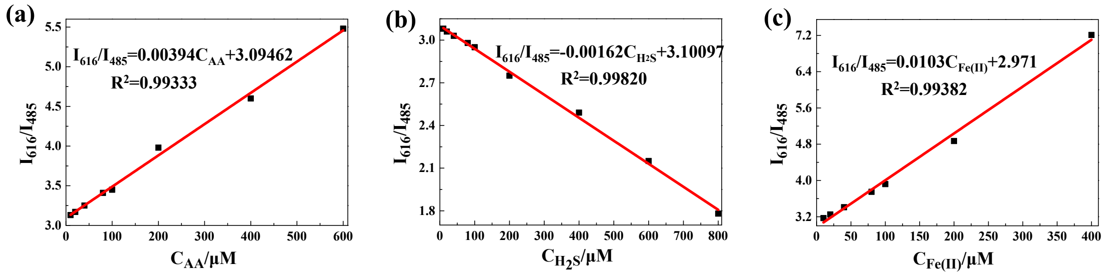

Fig. S9 Concentration dependence of the fluorescence intensity ratio (I_{616}/I_{485}) with (a) AA (0–600 μM), (b) H_2S (0–800 μM) and (c) Fe(II) (0–400 μM).

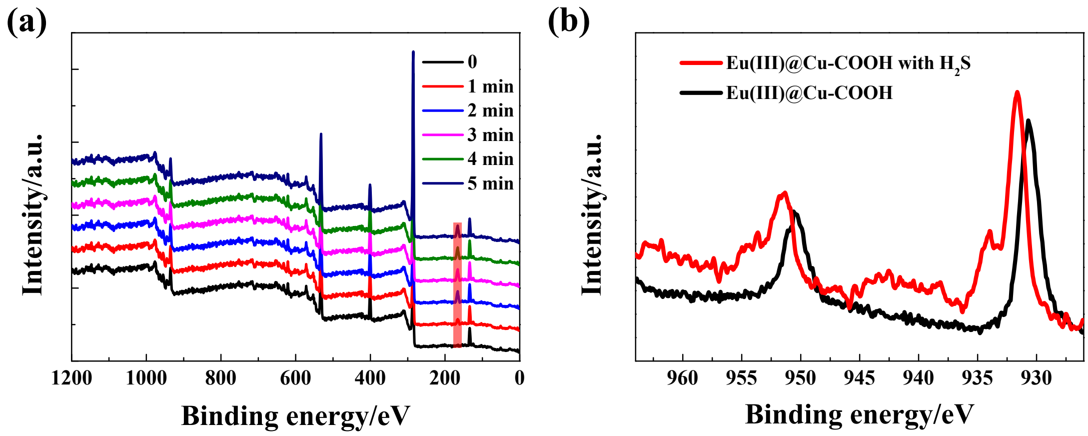

Fig. S10 (a) XPS spectra for Eu(III)@Cu-COOH with H_2S after 0-5min. (b) Cu 3p XPS for Eu(III)@Cu-COOH and Eu(III)@Cu-COOH with H_2S.

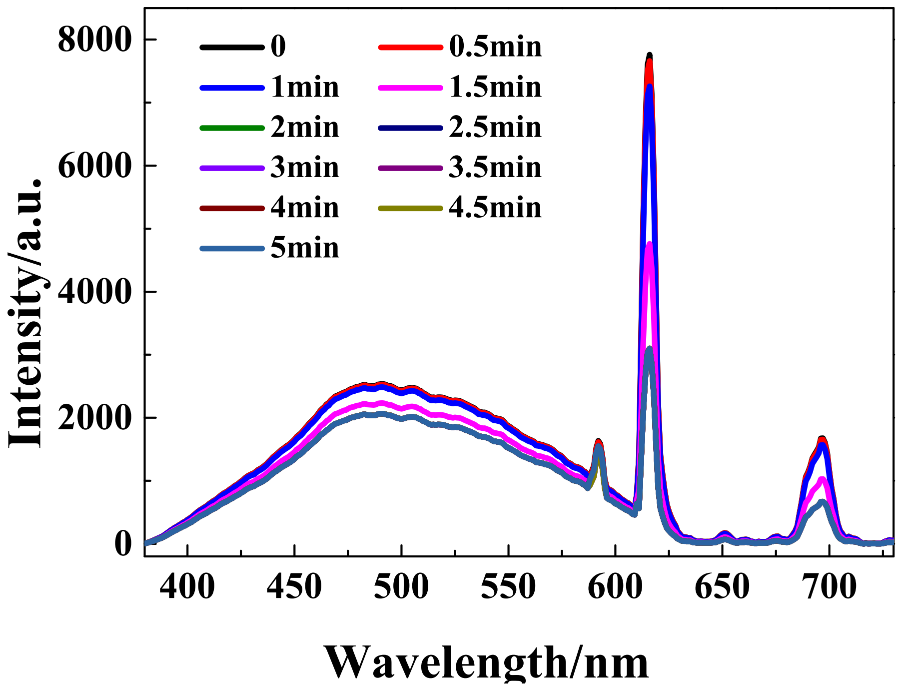

Fig. S11 Fluorescence spectra of Eu(III)@Cu-COOH towards addition of H_2S (2 mM) after 0-5 min.

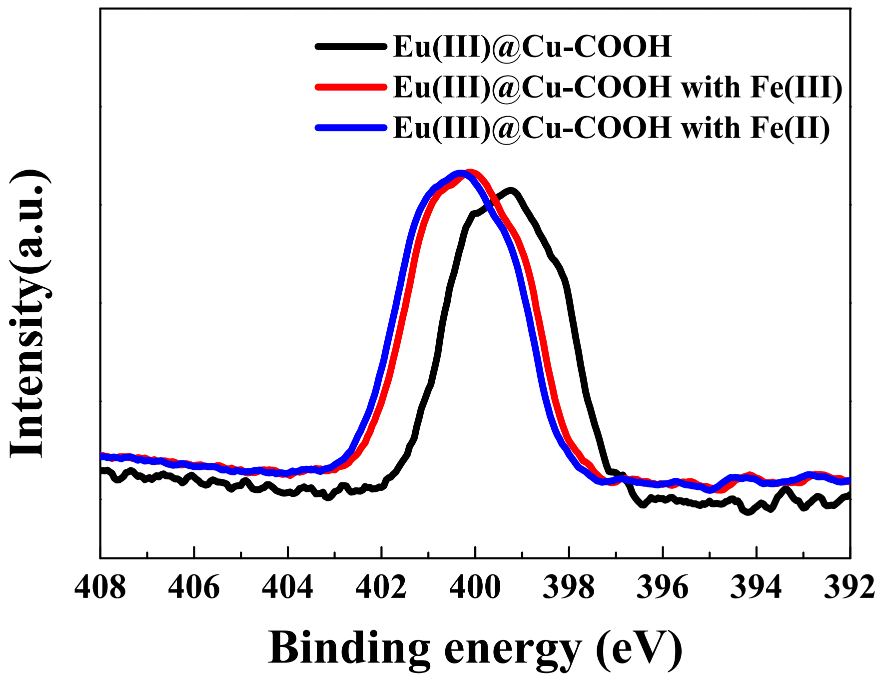

Fig. S12 N 1s XPS for Eu(III)@Cu-COOH, Eu(III)@Cu-COOH with Fe(II) and Eu(III)@Cu-COOH with Fe(III).

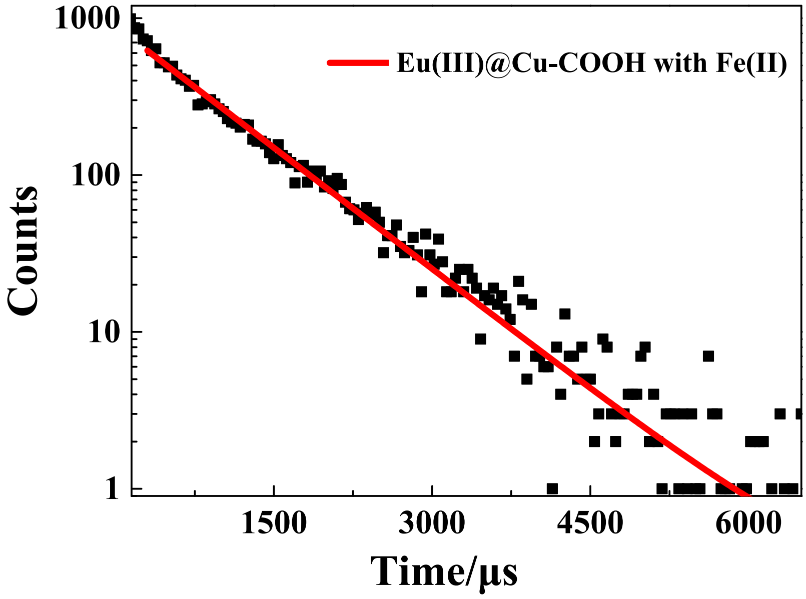

Fig. S13 Fluorescence decay curves of Eu(III)@Cu-COOH with Fe(II).

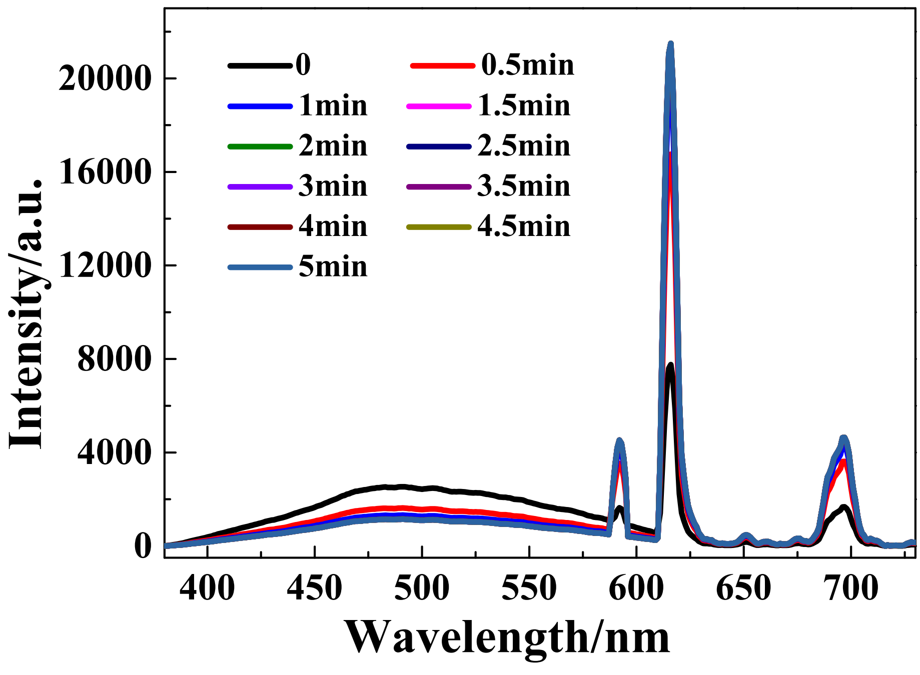

Fig. S14 Fluorescence spectra of Eu(III)@Cu-COOH towards addition of Fe(II) (2 mM) after 0-5 min.

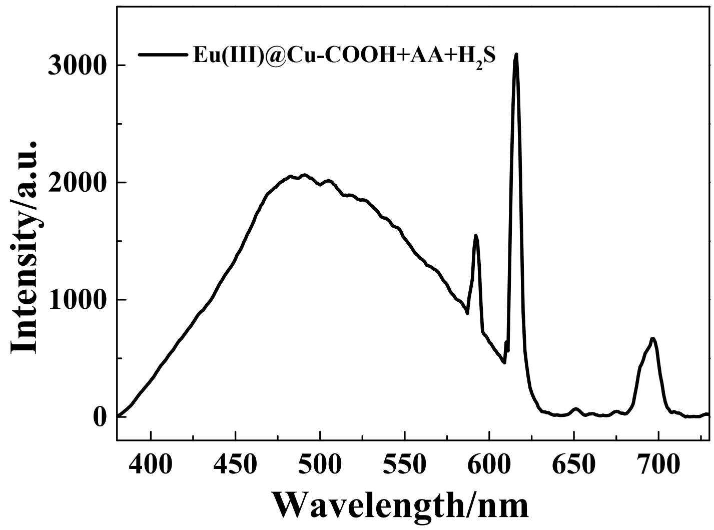

Fig. S15 Fluorescence response spectra of Eu(III)@Cu-COOH with AA/H_2S.

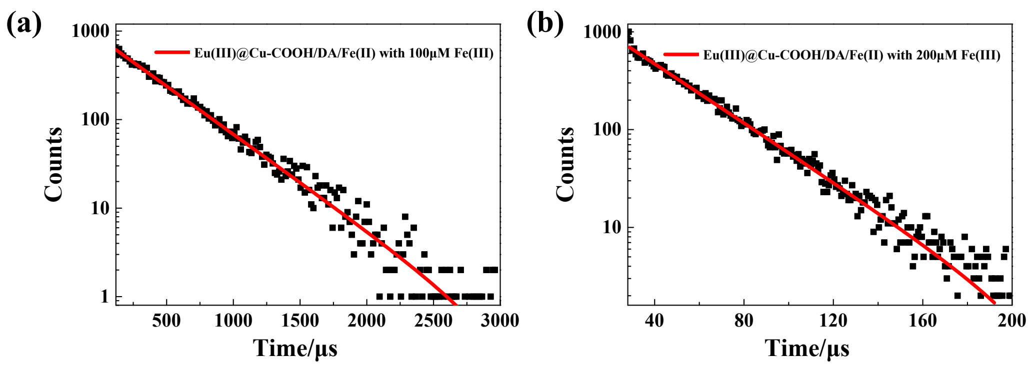

Fig. S16 Fluorescence decay curves of Eu(III)@Cu-COOH/DA/Fe(II) with Fe(III).